UNIVERSITY OF GÄVLE

FACULTY OF ENGINEERING AND SUSTAINABLE DEVELOPMENT

The methods of drag force measurement in wind tunnels

Li Nan

January 2013

Master's Thesis in Energy Systems

Acknowledgements

I would like to express my great sincere gratitude to my supervisor Professor Hans Wigö whose help, suggestions, never ending patience, and valuable and kind guidance brought me up to this achievement. During my thesis study, he spent lots of time on reading my drafts and gave many comments. It is not possible for me complete this study without his help.

A special thanks to Leif Claesson and Professor Mats Sandberg, with their help I could visit the laboratory of wind tunnel near the train station in central and I learnt a lot of knowledge about wind tunnels there.

I appreciate all the teachers had given the lectures in our department during the two years. From the basic to advanced, I have learnt a lot from them. It helped me to finish the final thesis perfectly.

I am also particularly grateful to my friends DouChang, Minhaz and Rubayet, they gave encouragement when I confused about my study. I got so much power from them and I love them.

Li Nan

Abstract

Different exist methods for measuring the drag force in wind tunnels have been presented in this study. The wall shear stress is one of the most important parameters during the drag force measurement. The techniques of the measurement can roughly be divided to two types which the floating-element balances and the hot-wire/hot-film anemometer. On the other hand, the methods also can be sorted by another way, direct methods and indirect methods. In this study, the direct methods are performed in more detailed.

The aims of this report are to analysis the exits methods and conclude the advantages and disadvantages of each method. In addition, some improvement suggestions are introduced scientifically.

For the direct methods, there are four methods have been described in this study. Earlier from 1993, Maruyama installed an element floating on water; in 2006, Mochizuki used a floating element with a mechanical device; in 2007, Cheng used an oil bath instead of water; and in 2010, Mats Sandberg and Hans Wigö measured drag force in the wind tunnels with a standard load cell. In addition, there is one advanced method can measure the drag force of each element in a large open area; however, it can also be performed in wind tunnels. The indirect method which is presented in this paper is based on optical techniques, and the oil-film interferometry technique has been used in this method.

Table of Contents

1. Introduction

The present thesis investigates to estimate the effects of drag force on different area densities in wind tunnels. It is necessary for many meteorological and wind engineering applications (design of building & structures), and also concerned with the dispersion of air pollutants, natural ventilation and heat transfer between the ground surface and the atmosphere. Further, the influence when the wind flow over open area from the view points of thermal comfort of the pedestrians [1]. In this situation, such studies may be described to improve the reliability of performance, economy of design or both of them.

Many experiments for measuring drag force in wind tunnels have been carried out to grasp the various aerodynamic effects in real environment. Such as, Maruyama used a floating element in the water bath which is not connected to the floor of the wind tunnel. Mochizuki installed a floating element to a mechanical device. While Gillies measured drag force on individual obstacles on a load cell. Cheng conducted the experiment using an oil bath with a raft. Mats Sandberg and Hans Wigö measured drag force in the wind tunnels with a standard load cell. Moreover, optical techniques as a low cost method are considered a good choice. The oil-film interferometry technique could be applied to estimate the drag force and it has been proved scientifically. The application of Irwin sensor plays an important role in drag force measurement experiment in wind tunnels because of the wind speed has a linear relationship with pressure differences.

Calibration plays an essential role in this study, since each setup cannot operate without calibration. It is an important issue that how to choose an efficient, appropriate as well as low cost calibration method. In this study, each procedure of calibration will be introduced detailed.

As a popular tool in modern times, CFD (Computational fluid dynamics) can contribute to calibrate the setup using for measuring the drag force in wind tunnels.

Fluid mechanics, however, is the main theory during the whole study. Therefore, in the theory part, amount of concerned definitions and equations have been presented clearly.

2. Theory

2.1 Aerodynamics force

It occurs on a body is immersed by the fluid or some other gas. The relative movement between the body and the gas caused the aerodynamics force.

The force could be generated on the surface of the body owing to pressure and viscosity [2][3][4]. The figure below shows the force on an aerofoil.
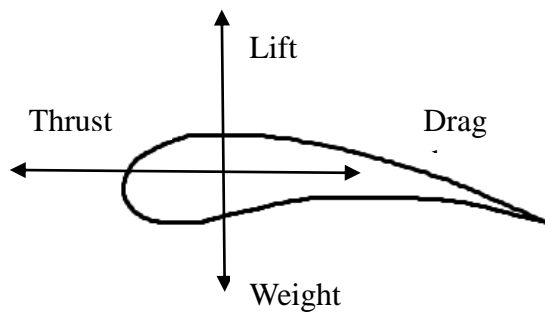

Fig.1. Forces on an aerofoil

2.2 Drag and lift

2.2.1 Drag force

Drag force can be defined as in fluid mechanics, the force which exerted on the solid object in the upstream direction of the relative flow velocity [9] [10].

Drag force depends on flow velocity and it decreases the fluid velocity [11]. Therefore, drag force also called air resistance or fluid resistance.

2.2.2 Lift force

Contrasts with the drag force, lift force exerts when a fluid flowing pass through the surface of an object and the direction of lift is perpendicular to the flow velocity direction [12]. The following figures show the drag and lift force;
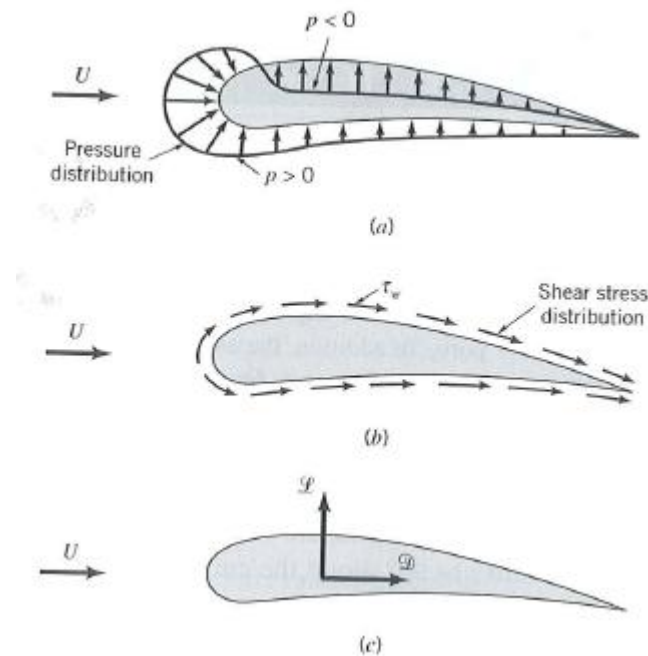
Fig.2.Forces from the surrounding fluid on a two-dimensional object: (a) pressure force, (b) viscous force, (c) resultant force (lift and drag)[45].
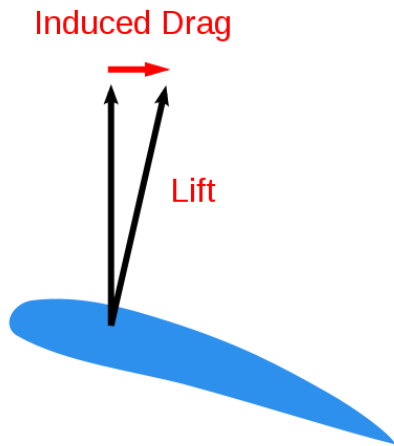
Fig.3.The relationship between drag and lift force [5] [6].

2.3 Viscosity

Viscosity is a factor that the fluid is deformed by the either shear stresses or tensile stress. For fluids, the viscosity of water is low; the viscosity of honey is higher than water. Simplicity, the fluid with less viscous has easier movement [7]. The following figure shows the viscosity of pitch and water.

Fig.4. Pitch has a viscosity approximately 230 billion (2.3×1011) times that of water [8]

2.4 Wall shear stresses and normal stresses

Wall shear stresses τ occur on the object interface when the object moves through a fluid. The wall shear stresses due to viscous effects and the normal stresses due to the pressure p.

The relationship between shear stresses and drag force can be described by following equation:

$$\tau = \frac{F}{A} \tag{1}$$

Where τ is the shear stress

F is the drag force

A is the cross-sectional area of material with area parallel to the applied force vector.

2.5 Drag coefficient

Drag coefficient is one of the most important factors in the field of fluid mechanics. It is often used in the drag equation. It is proportional to the drag force which act on the body immersed in the fluid; namely, less drag coefficient indicate less drag force.

Drag coefficient usually interrelated with a particular surface area [13].

The equation of drag coefficient is defined as;

$$C_d = \frac{2F}{\rho v^2 A} \tag{2}$$

Where F is the drag force

ρ   is the mass density of the fluid

v is the speed of the object relative to the fluid

A is the reference area.

2.6 Wind tunnels

2.6.1 General imagine of wind tunnels

A wind tunnel which is a duct contains air flow or other gas. It is usually used to study about the flow past the models of aircraft, structures and vehicles, etc. There are many types of wind tunnels in the world which with different scales [14][15][16][17][18][19].
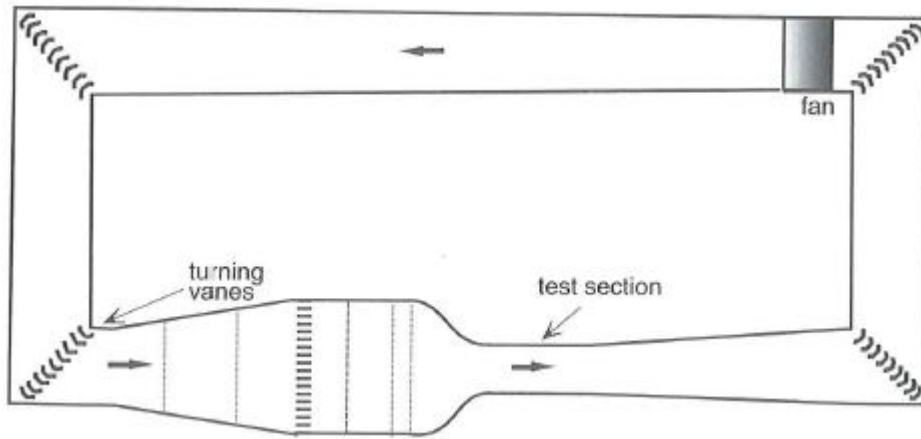
The wind tunnels used for general purpose can be designed and built with moderate amount of effort and resources [20][21][22][23].

2.6.2 Low-speed wind tunnels

Low-speed wind tunnels means the maximum speed of the wind tunnels would be lower than about 100m/s and the compressibility effects which caused by pressure would be negligible.
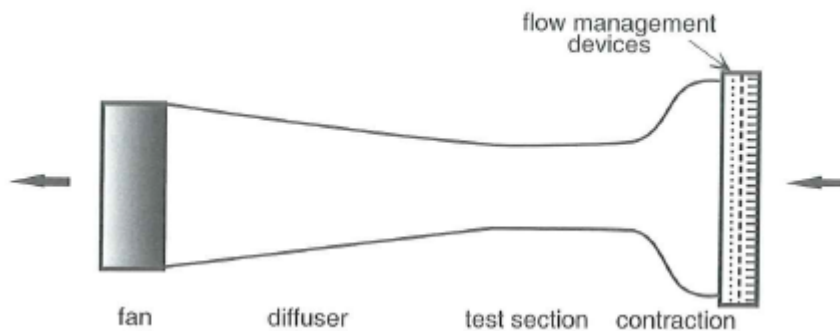
2.6.3 Closed-circuit wind tunnels

Fig.5.Closed-circuit wind tunnels [46].

As the *Fig.5* shows, most large wind tunnels are designed to closed-circuit wind tunnels because compared with open-circuit tunnels; they have much higher power efficiency, lower noise levels and flow containment, and easy to control the flow.

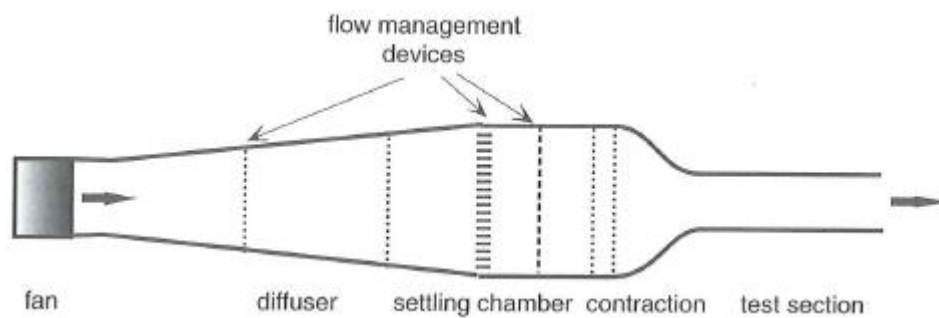## 2.6.4 Suction wind tunnels

Fig.6. Suction wind tunnels[46].

Suction wind tunnels are arranged in a straight-line and open-circuit. First, the air flow passes through an air filter, a honeycomb and screens. Then, enters the contraction part which leads to the test section.

Less cost to build, less occupy laboratory space and easier to design are the advantages of

suction wind tunnels. However, the free of disturbances caused by an upstream fan due to external obstructions and wide range recirculation in the laboratory.

2.6.5 Blowdown wind tunnels

Fig.7.Bowdown wind tunnels [46].

Difference with suction wind tunnels, the fan is arranged upstream of the test section. Such a design, in a certain extent, improves the flow control compared with suction wind tunnels.

Overall, open-circuit wind tunnels subjected to contamination due to they are freely communicate with their surrounding space even it is in an enclosed laboratory.

2.7 Wind and Its Origin

Wind is the air movement from higher pressure to lower pressure. Briefly, it is caused by different pressure in the atmosphere. The wind is much slower near the Earth's surface than otherwise due to the friction [24].

2.8 Reynolds Number

The Reynolds number (Re) is the ratio of inertial forces to viscous forces and it is a dimensionless number. Initially, George Gabriel Stokes introduced the concept of Reynolds number in 1851 [25], however, the name was given by Osborne Reynolds (1842–1912), who popularized its use in 1883 [26] [27].

Reynolds number as an essential factor in fluid mechanics, it would explain the different regimes such as laminar (or streamline) and turbulent flow: when the Reynolds number is low, the viscous forces are dominant, the flow which named laminar flow goes steady and smooth, in contrast, if the Reynolds number is high, the inertial forces are dominant, the flow which named turbulent flow tend to generate chaotic eddies, vortices and other flow instabilities. The figure below shows the character of the steady, viscous flow past a flat plate parallel to the upstream velocity.
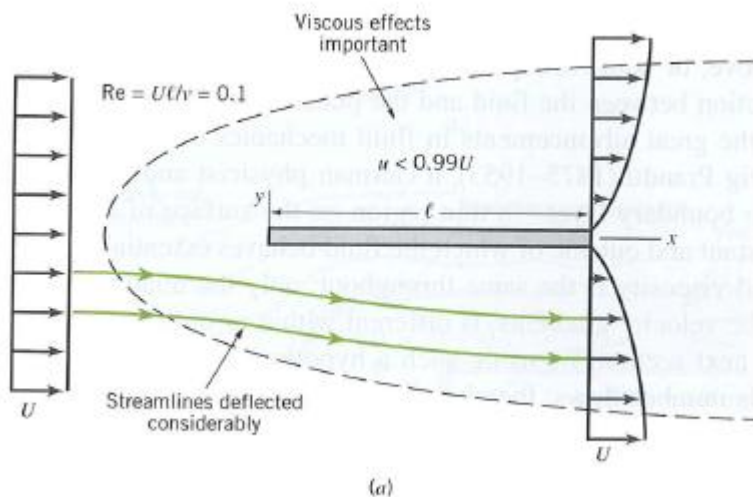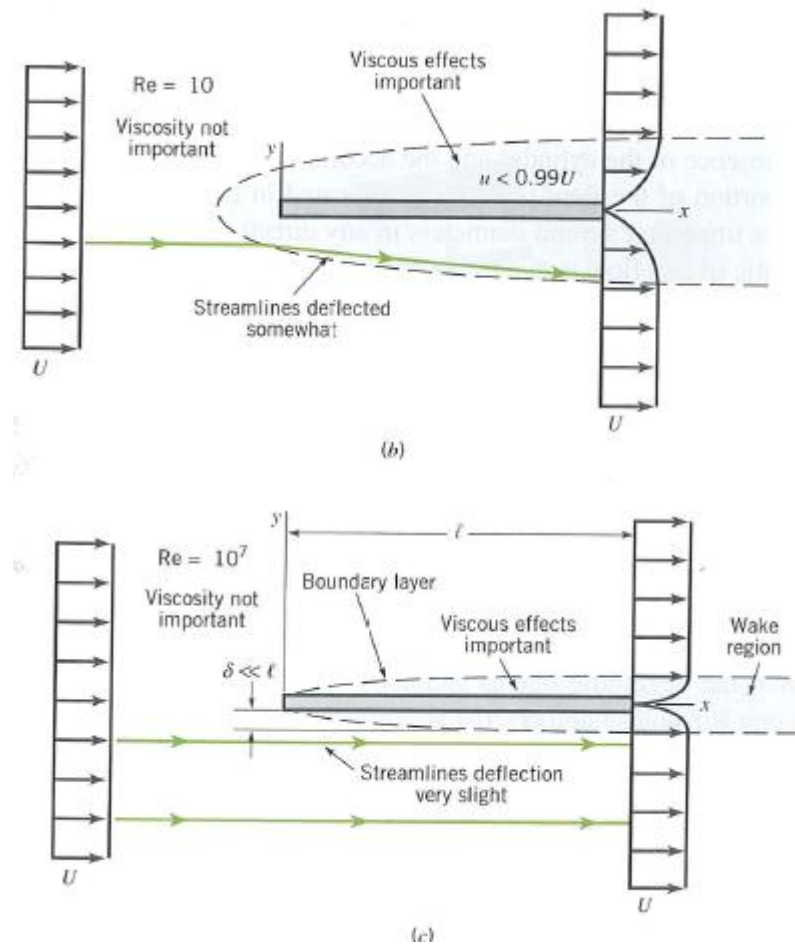
Fig.8.Character of the steady, viscous flow past a flat plate parallel to the upstream velocity: (a) low Reynolds number flow, (b) moderate Reynolds number flow, (c) large Reynolds number flow [45].
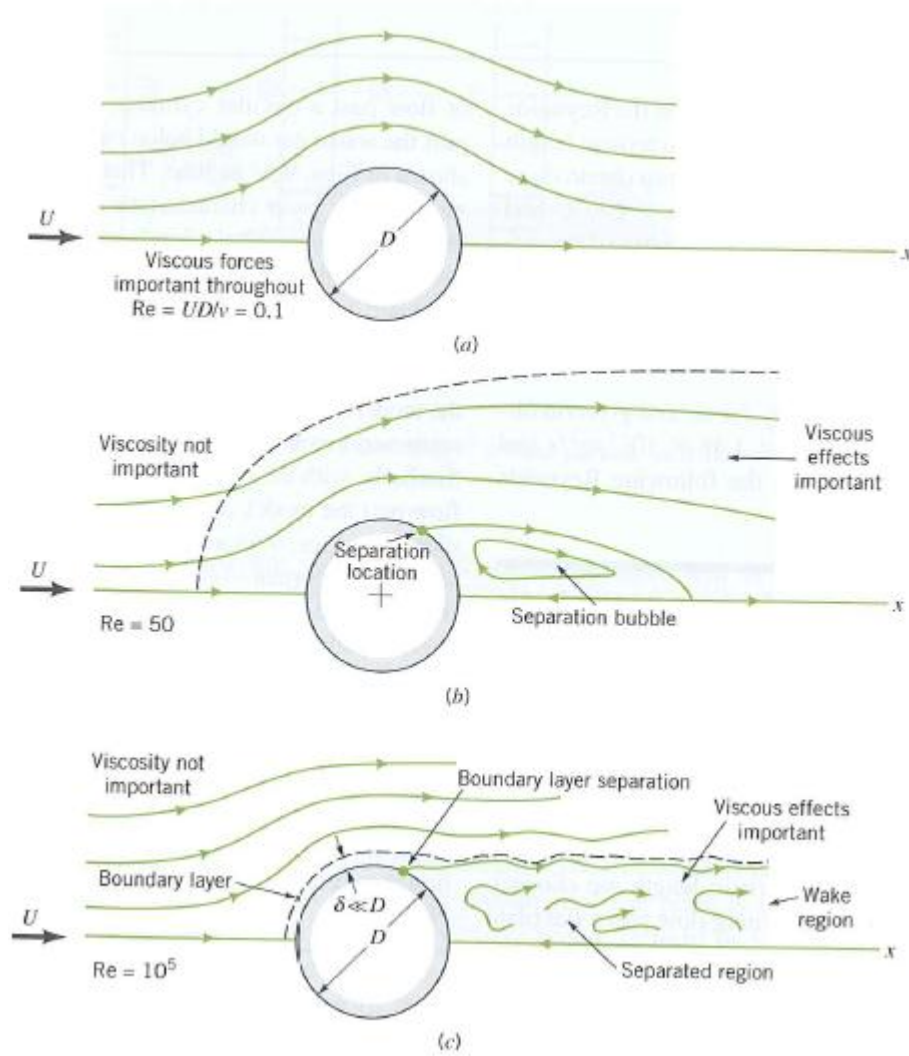
Fig.9. Character of the steady, viscous flow past a circular cylinder: (a) low Reynolds number flow, (b) moderate Reynolds number flow, (c)large Reynolds number flow[45].
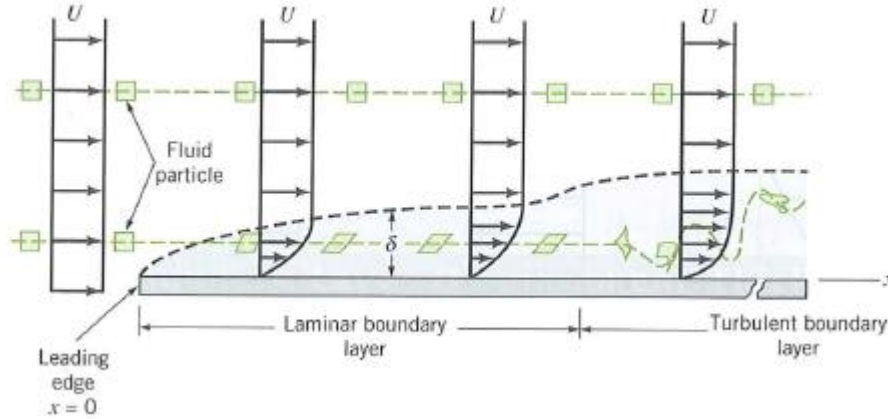
2.9 Boundary layer

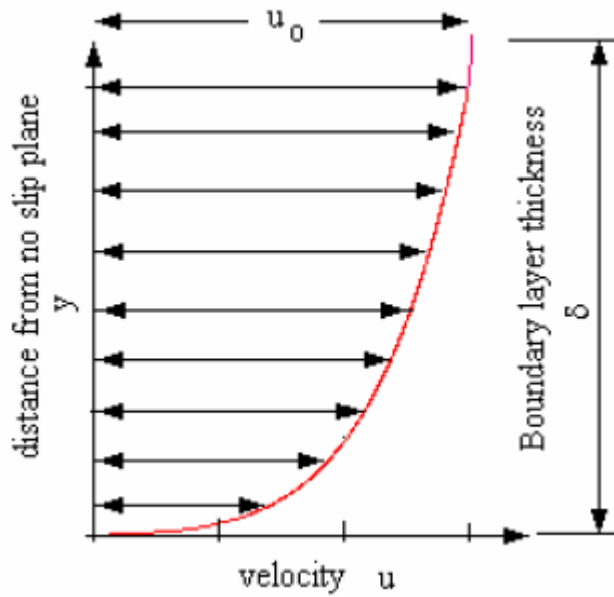*Fig.10. Distortion of a fluid particle as it flows within the boundary layer [45].*

Fig.11.Typical boundary layer [28].

As the *Fig 11* shows, the velocity of the flow u increases with the height y. When the distance required for the velocity reach 99% of u_0,the layer is called boundary layer ,δ is called boundary layer thickness [28].

2.10 Skin friction

Skin friction arises from the friction between the surface of the object and the fluid when the object moves through the fluid.

The relationship of skin friction coefficient and the wall shear stress is defined by;

$$C_f = \frac{\tau_w}{\frac{1}{2}\rho U_\infty^2} \tag{3}$$

Where C_f is the skin friction coefficient

τ_w is the local wall shear stress

ρ is the fluid density and

U_∞ is the free-stream velocity.

3. Methods and discussions
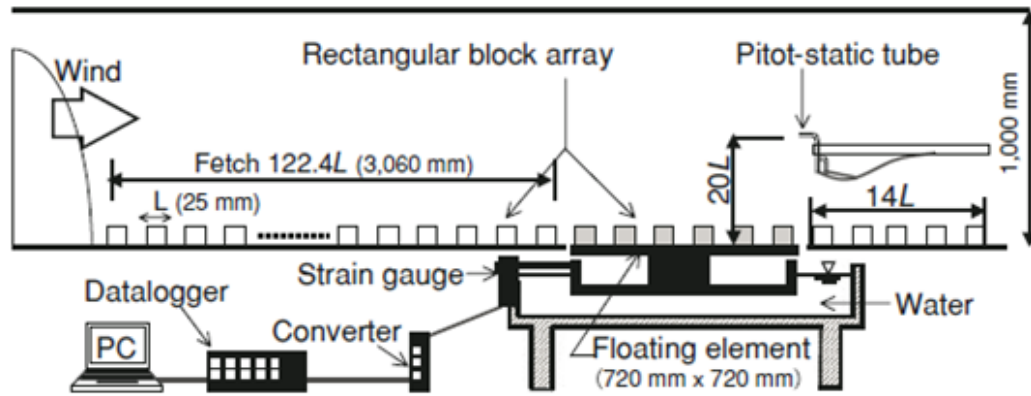
3.1 Floating-element on water bath
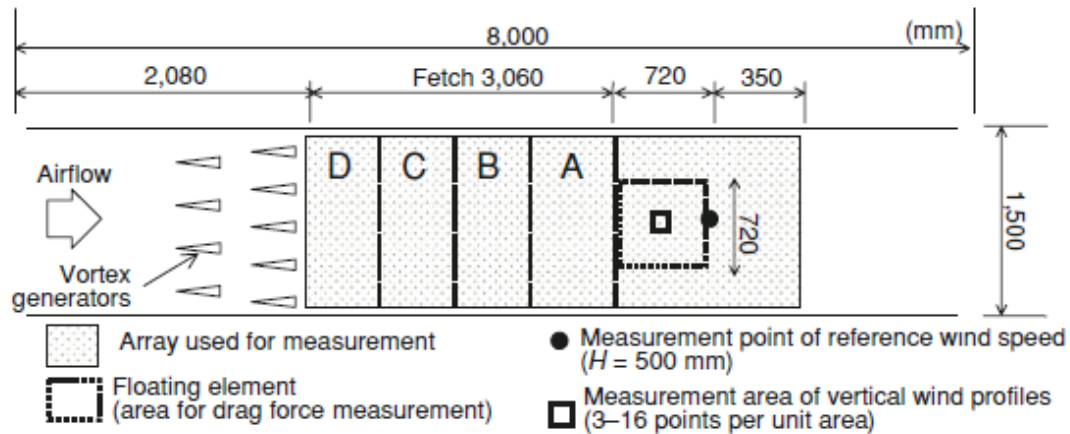
Fig.12.Side view of method set-up [1].

Fig.13.Schematic plan view of the wind tunnel [1].

Background:

As early as 1993, Maruyama had used en element floating on the water bath to measure the drag force. The experiment was conducted at the Interdisciplinary Graduate School of Engineering sciences, Kyushu University, Japan.

Description:

The method was performed in the low speed, closed-circuit wind tunnel which has the test section with height 1m, length 8m and width 1.5m [30]. The leeward point which used to measure wind speed and drag force was almost 3 m from the spires of the wind tunnel, as shown in Fig12 and Fig 13. In the square cavity of the floor of the wind tunnel, the floating element was arranged, which with dimension of 720mm×720 mm.

For the lowest density (4.3%), 36 rectangular blocks were stands on the floating element. These blocks should be the same in size and it's improved the accuracy of a large drag force measurement. Drag measured on a span-wise single cube has variability about 10% [29]. Hence, using a large floating element with great amount of blocks could provide a higher accurate measurement of the drag force.

The floating element was adjusted before the experiment performed. The top of the surface should be the same level as the wind tunnel floor and it was separated by 2mm on all sides from the tunnel floor and. That means it was mechanically isolated from the wind tunnel and that the force of the floating element was only due to air resistance. The floating element and the surrounding floor of wind tunnel were covered by the same arrays blocks. The lengths of surrounding floor were 3m and .35 m, which in windward and leeward directions. That made the fetch 120 times standard blocks size L. Each L should be 25 mm.

Adjustment and Calibration:

Strain gauge was used to measure total drag force in this method directly. Its measurement resolution was better than 7.4×10^{-4} N and 0.4% of the minimum drag measured in this study.

Strain gauge is a device used to measure the strain of an object. The calibration is required to assure the accuracy of the instrument, and also scale the instrument sensitivity is necessary.

Basically there are two methods for calibrate the strain gauge, direct and indirect. With direct method, one precisely known mechanical input is applied to the sensing elements of the

measurement system, and then the output of the instrument is compared to the known input for verification purposes. For the indirect calibration, special equipment and facilities are required for valid implementation, so this method is not used widely for typical stress analysis laboratory. Overall, more practical and ordinary used to approach to either instrument verification or scaling is by direct calibration.

In this experiment, the system adjudgment was processed by following steps;

At first the device was reset to zero. Before each run the measured value for 150s under zero-flow conditions was applied. Then the drag force was measured with stream velocity 8 ms^{-1} for 300 s. After then again measured the same procedure for 150 s under zero flow conditions with negligible elastic hysteresis effect. The total procedure of each run needed 600s. This process was repeated five times for each array and takes the average value as the result of this study. It was accepted that the variation below 0.2% for all cases [1].

Advantages:

1. Air leakage was prevented by using water as the floating liquid. For this system, theoretically zero internal friction was approved.
2. Low cost facility was used in this method, as well as the strain gauge.
3. It was quite easy to be conducted in the laboratory or any enclosed space.
4. Because the strain gauge measured the drag force directly, thus, the complex calculation process was not needed. It provided high efficiency.
5. Since the distance between the floating element and the edge of the bath which filled with water was large enough. Therefore, capillary force could not influence on the result of the experiment.
6. Due to low speed wind tunnel, the noise pollution was very low compared with   the high speed wind tunnels.
7. No air pollution was produced during the experiment. It was an environment friendly method.

Disadvantages:

1. In this method, water was used as the floating liquid. Since water has lower viscosity, the damping oscillation of the floating element might affect the result during the experiment.
2. The process to calibrate the strain gauge is complex. For each array the calibration need 600s.
3. Spatial and temporal resolutions are relatively low.
4. High sensitivity with the surrounding clearance size and the floating element surface.

Improvement suggestions:
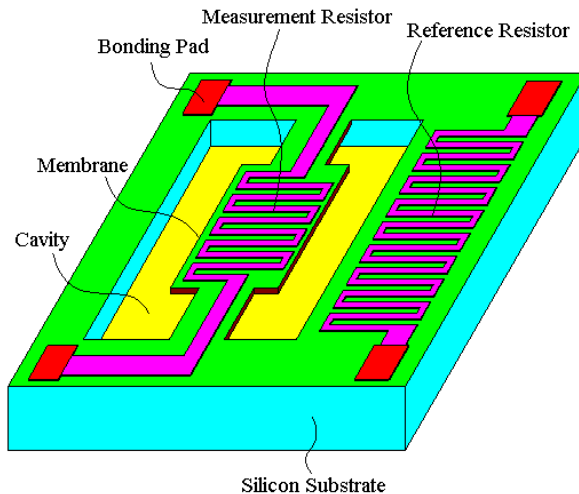
Fig 14.MEMS sensor [48].

Recently, the silicon micromachining technology (MEMS short for (MicroElectroMechanical Systems) has been used to instead of the traditional sensors in the floating-element experiment, as the Fig14 shown. They have smaller size than conventional sensors and also they have lower error rate since they are integrated [31].

The size of MEMS devices generally range from 20 micrometers to a millimeter. MEMS are made up of components between 1 to 100 micrometers in size. They usually consist of a central unit that processes data (the microprocessor) and several components that interact with the outside such as micro sensors.

The benefits of using MEMS include:

1. The lower cost during the batch fabrication.

2. Minimal disturbance due to the small size as human pupil.

3. Power requirements are very low.

3.2 Floating element with a mechanical device

Background:

In 2006, Mochizuki S, Kameda T, Osaka H measured the shear stress using the floating element with a mechanical device. This experiment was performed in department of Mechanical Engineering, Yamaguchi University, Japan.
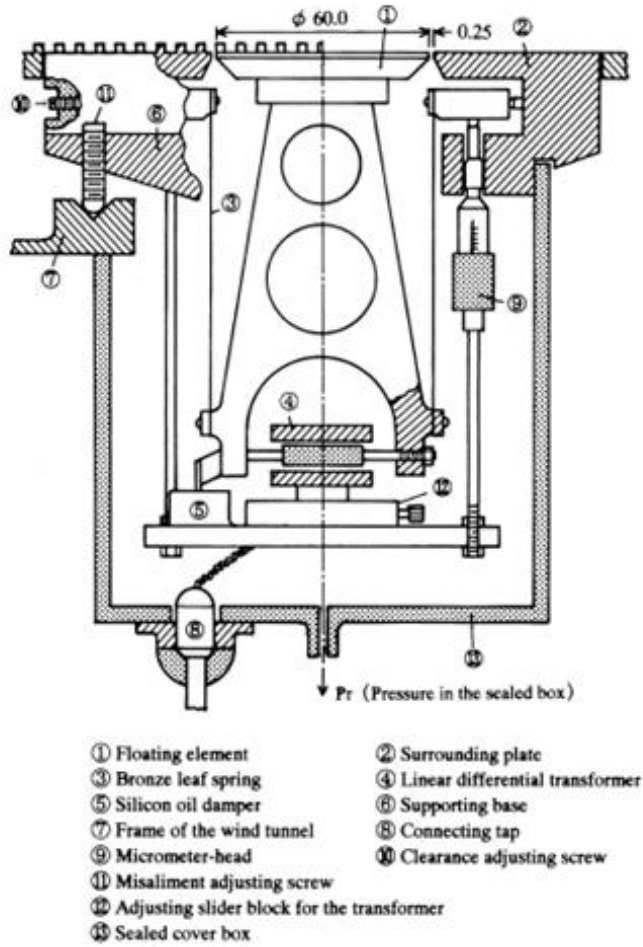
Description:

Fig.15. The device used in this method [31].

In this method, the shear stress acting on the rough surface was measured by the device directly. The circular floating element with a diameter 60 mm and 10 roughness elements attached were held in the middle of the device by two bronze links. And the gap between the floating element and the surrounding plate is 0.25 mm which is much larger than the viscous wall length; the disturbance of the flow because of the gap could be ignored [32].

It is clear to see the schematic of the flow field. And the wind tunnel in this study is a low-turbulence wind tunnel with 300*500 mm^2 in width and height and 4 meters in length.

Calibration:

The device can be calibrated as follows;

A known load used in the calibration was hanged in the thread which on the surrounding plate; a horizontal force was generated and acting on the floating element. Due to the linearity of the system is high; the output was proportional to the input value, that is, the displacement of the floating element in this experiment was proportional to the load, as shown in Fig 16. When the displayed data is consistent with the load acting on the thread, the system was ready and can be used.

The obtained calibration curve has very good linearity simplicity as shown in *Fig.16*.
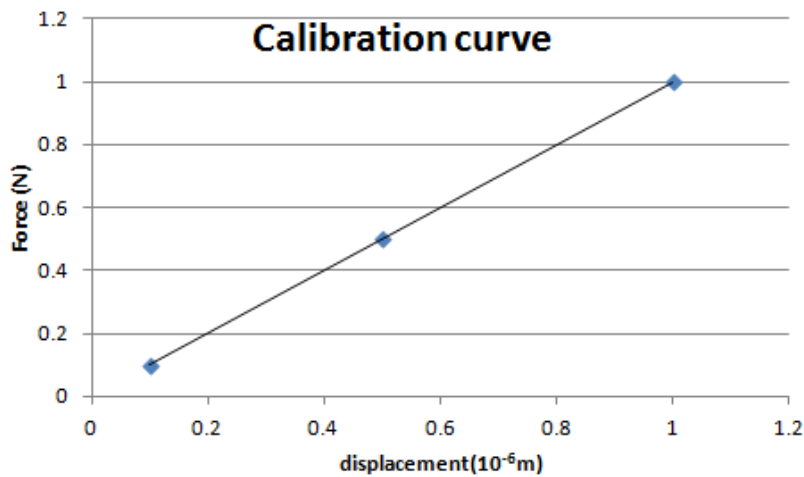
Fig.16. Calibration curve

<u>*Advantages:*</u>

1. Calibration is easy to be performed.
2. The accuracy of the method is pretty high, as the linear differential transducer can detect displacements to 0.1 μm.
3. Wall shear stress could be measured directly.

<u>*Disadvantages:*</u>

1. High cost facility was applied.

2. The obtained data could be affected by the internal friction caused by air leakage.

3. The floating element needed to be adjusted to keep the same level with surrounding plate surface before each run.

3.3 Floating-element on oil bath

<u>Background:</u>

H.Cheng had measured the drag force using the floating element balance from 2006 to 2007. The experiment was conducted in EnElo, School of Engineering,, University of Surrey, UK. Compared to the method by Maruyama in 1993, H.Cheng used the oil bath instead of the water bath.

<u>Description:</u>

The wind tunnel used in this method with the test section 4.5 m long, 0.6 m high & 0.9 m wide. Density of two area (ratio between plan area and occupied by the roughness elements) coverage is 25% & 6.25% respectively as shown in *Fig.17*.
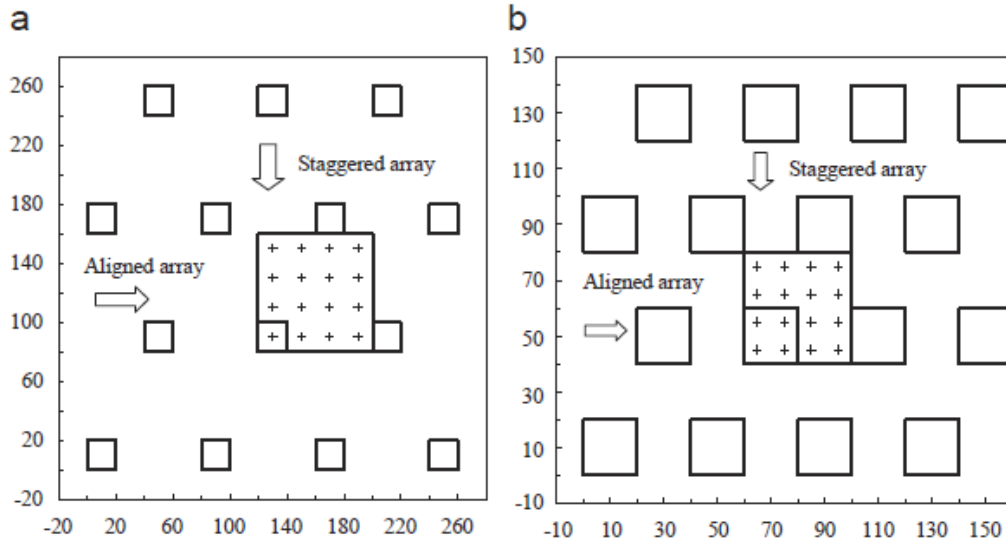
Fig.17. Schematic diagram of the roughness surface: (a) 6.25% cube array, (b) 25% cube array [33]

In the figure, cubes are stands in staggered and aligned patterns. When the wind comes from top to bottom they are staggered or comes left to right cubes are aligned.

The roughness elements are sharp edged wooden cubes with side 20 mm. The rough surface was raised by 60 mm above the tunnel floor in order to avoid the interference of the boundary layer. The total experiments were performed on the tunnel centerline and almost 3m downstream of the roughness leading edge. Drag measurements were performed 4-10 ms^{-1} free stream velocity.
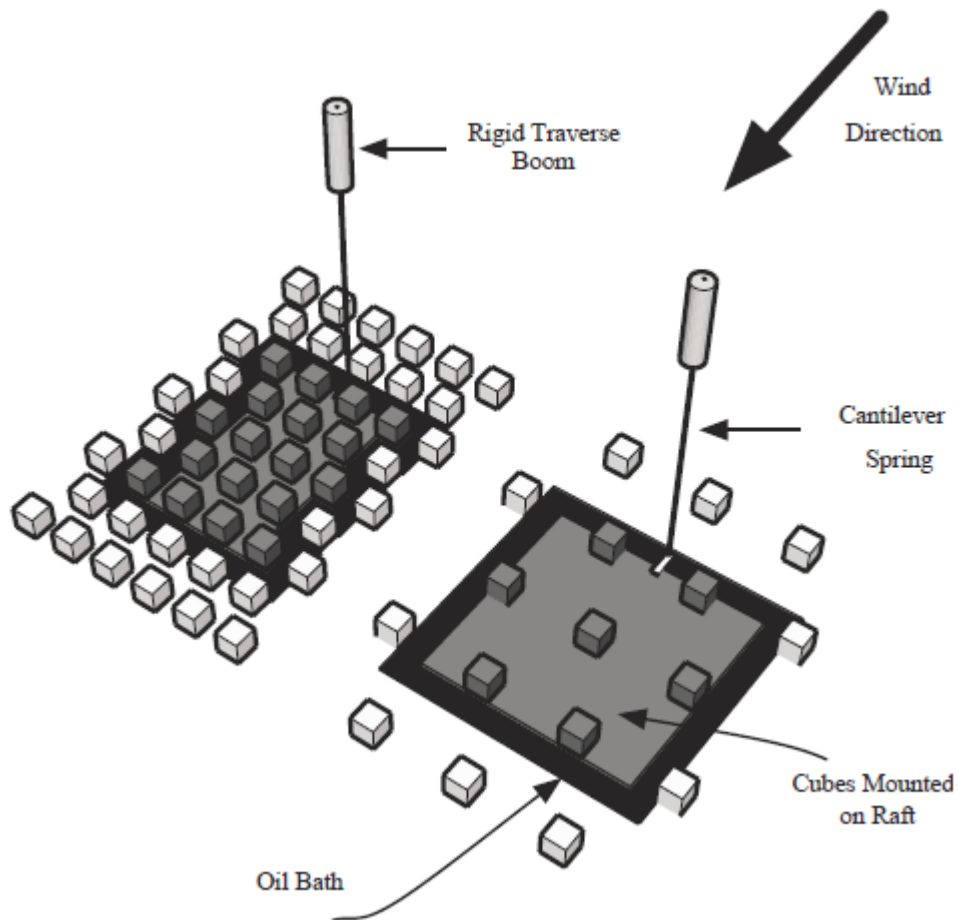
Fig.18.25% and 6.25% roughness array on a raft. [33].

The measurement of total surface drag depends on floating drag balance. The roughness elements, 18 for 25% surfaces and 7 for 6.25% surfaces stand in the same pattern of roughness array on a 'raft' as shown in *Fig.18*.

Raft was placed in the oil bath. It was located on the tunnel centre-line 3m downstream of the leading edge of the roughness array. Bath plan area was larger than raft, so there was 20mm gap between the raft and the edge of the bath. These 20mm gap prevents surface tension of the raft to be attracted of bath edges. The buoyancy of the raft was designed that the top of foam surface was just above the oil level. When the bath was filled with oil, cube height was same to the surrounding array.

EP80 gear oil was selected for this experiment. Its high viscosity was useful for damping

oscillation of the raft. The viscosity prevents the oil surface becoming disconcerted by the moving air. Air leakage was prevented by floating the raft. So that it is theoretically zero internal friction in this system.

The raft was joined to the vertical tube, which was held by the overhead traversing system shown in *Fig.18*. Its longitudinal position was adjusted to maintain the correct position of raft relative to the surrounding array. The aerodynamic drag force acting on the cube and raft surface can be obtained by measuring the cantilever deflection (through the change in traverse position). The range of tunnel speeds was from 4 to 12 ms^{-1}. The firmness of the cantilever spring was calibrated before the experiments.

Adjustment and Calibration:

1. The top surface of the raft should be arranged just above the oil level, so that when the bath was filled with oil, the cubes on the raft had the same height with the surrounding array.
2. The stiffness of the cantilever spring needed to be calibrated before the experiments started.
3. As like the second method mentioned in present paper, the linearity relationship between the change in traverse position and drag force obtained in the experiments used in the calibration. The similar procedure was performed in this method.

Advantages:

1. EP80 gear oil was applied in this method due to the high viscosity. Hence, the damping oscillation can be avoided during the experiments relatively.
2. Air leakage was prevented by using the floating on the oil bath.
3. The large gap between the raft and the edges used to avoid the raft to be attracted to the bath edges by surface tension.
4. Because of the high viscosity oil, it was not too perturbed by the surrounding air.

5.   The test section dimension of the wind tunnel was quite small; the experiment can be conducted in the normal laboratory and factory.

6.   Low cost had been used in the method.

Disadvantages:

Calibration process was complex relatively.

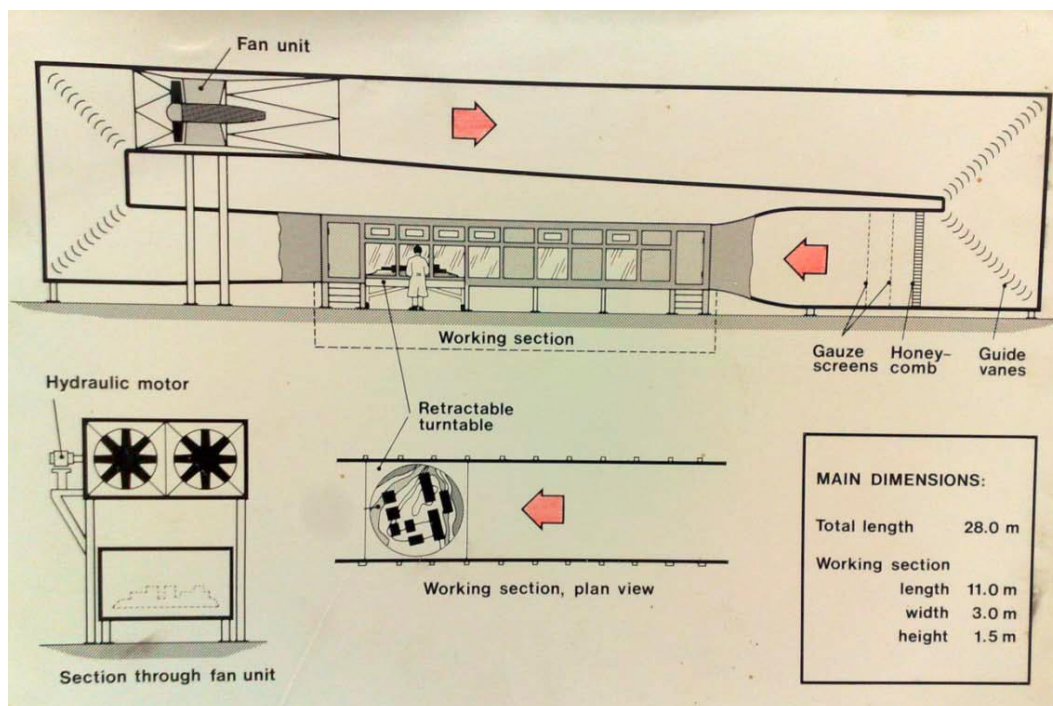### *3.4 Drag force measured by the load cell in wind tunnel*
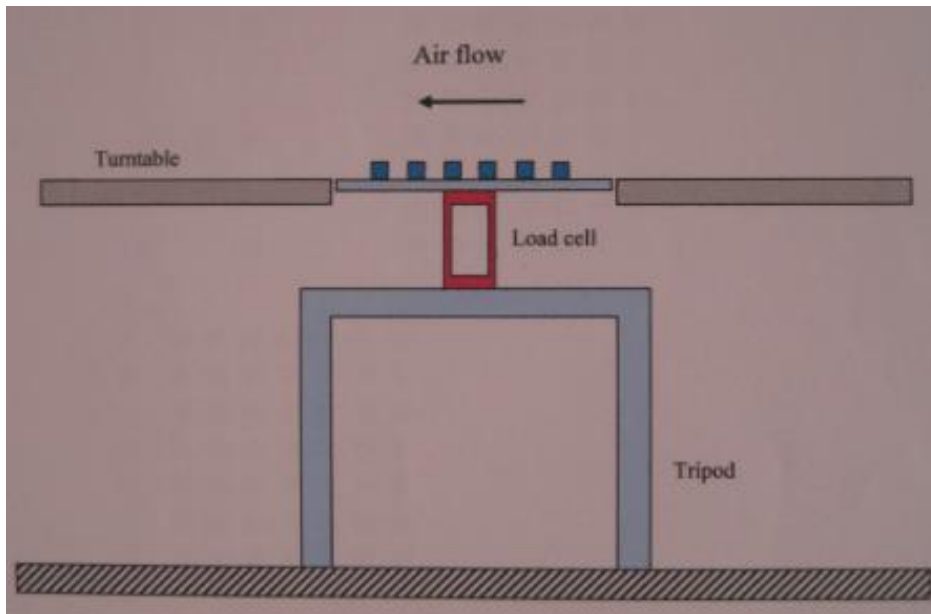
Fig.19. The view of the wind tunnel

Background:

In 2010, the professors of G ä vle University Sandberg M, Wig ö H measured the drag force using the load cell in the wind tunnel.

Description:

Fig.20. Schematic of a wind tunnel in HIG

Fig.20. showed the schematic of the wind tunnel of HIG and its properties. This was a closed-circuit wind tunnel with a maximum wind speed of 22m/s which was provided by two 1.5m diameter axial flow fans. It can be seen that the length of working section of this wind tunnel is 11m, the width is 3.0m, the height is 1.5m, and the total length of wind tunnel is 28 m.

Fig.21. Side view of drag force measuring principle

Fig.21. showed that the setup of the working section of the experiment. The objects located on the turntable in the wind tunnel and the disc was connected with a standard load cell which was mounted on a stable tripod on the floor of the laboratory hall. The objects were attached to the disc which has the same level with the turntable. The gap between the turntable and the disc was about 1mm. It means the disc was completely separated from the wind tunnel [34].

The aim of the experiment was to measure the drag force acting on models of building blocks with different packing densities. But when the blocks density was changed, the calibration had to been done again due to the fact that the system was very sensitive [34].

Calibration:

Calibration is needed before the experiment is conducted.
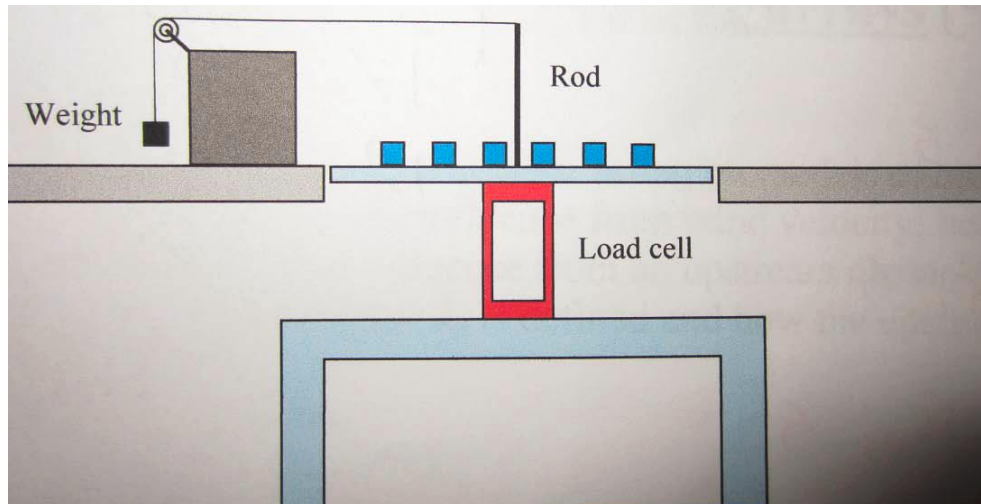
Fig.22. Calibration setup

The first step in the measurement process is calibration. Calibrating the measurement system can be accomplished by means of a mass hanging in the thread. Fig22 showed calibration setup of the experiment. Known mass which was 100 gram in this experiment has been applied. When displayed value is consistent with the weight, system is calibrated and ready to use. In this case, error of measurement would be deducted as much as possible.

Advantages:

1.   The load cell measured the force in only one direction which the air flow direction in the wind tunnel. So where the force attacked the blocks can be ignored, because the load cell was not sensitive to any torque.

2.   Calibration was easy to be conducted.

Disadvantage:

The load cell is very sensitive. Calibration is needed before the block configuration is changed on the disc.

3.5 Individual drag force measurement

Fig.23. the view of the drag balance mechanism [35].

Background:

Different from the methods presented previous, this method is quite special as it made individual drag force measurements available. However, it was not conducted in wind tunnels but in an large open field. In 2006, John A.Gillies, William G.Nickling, James King performed this experiment which aimed to measure the total shear stress acting the surfaces, the surface shear stresses on the ground between the elements and the drag force of each element.

Description:
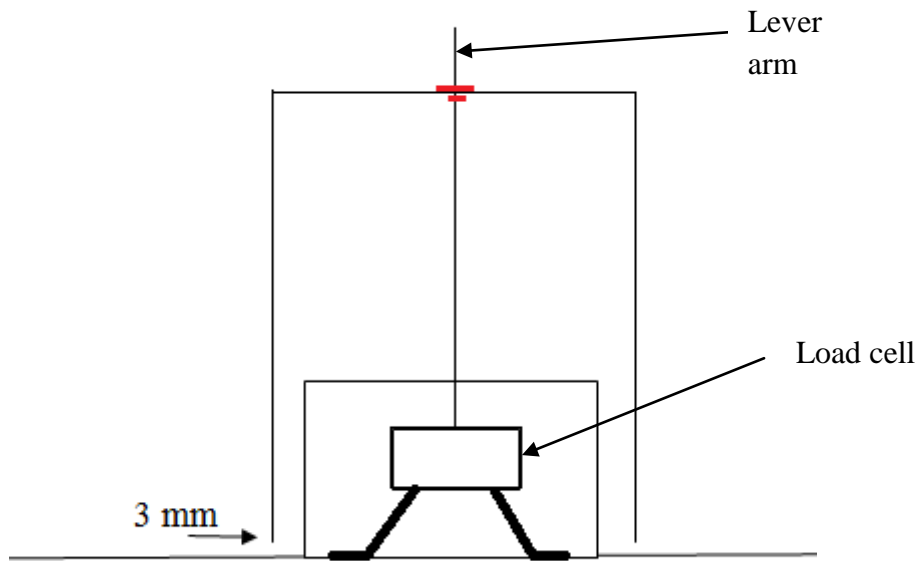
Fig.24.The intuition view of drag balance

As the *Fig.24.*showed, the principle of measuring the drag force on individual element is the force is transferred through a lever arm to a sensitive load cell which was fixed on one end to the ground and on the other end to the lever arm. So that the force would compress the load cell by pressing the lever arm and bucket.

In this method, Drag balances were potted inside boxes and stood in the roughness array by covering the box. In the top of the box there is a hole. A threaded rod passed through the box and the center of the bucket. The box was fixed to the lever arms which provided access to attachment point for the roughness elements.

The bucket was also fixed to the lever arms using a threaded rod locked with a washer and nut, which can allow it in free movements. After fixed it bucket was slightly above to the surface (3 mm).
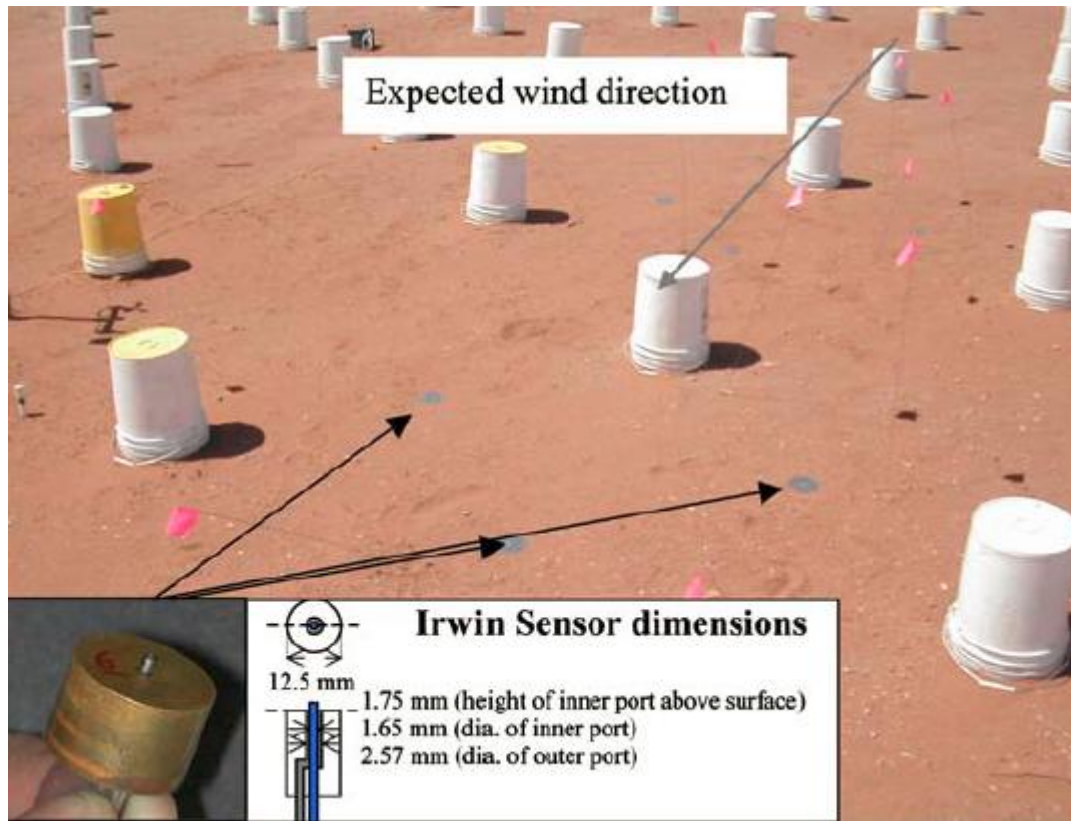
Fig.25. the view of the setup of the experiment [35]

The second task in this experiment is to measure the surface shear stress in each array.

In addition, different density arrays had been applied in the experiments.
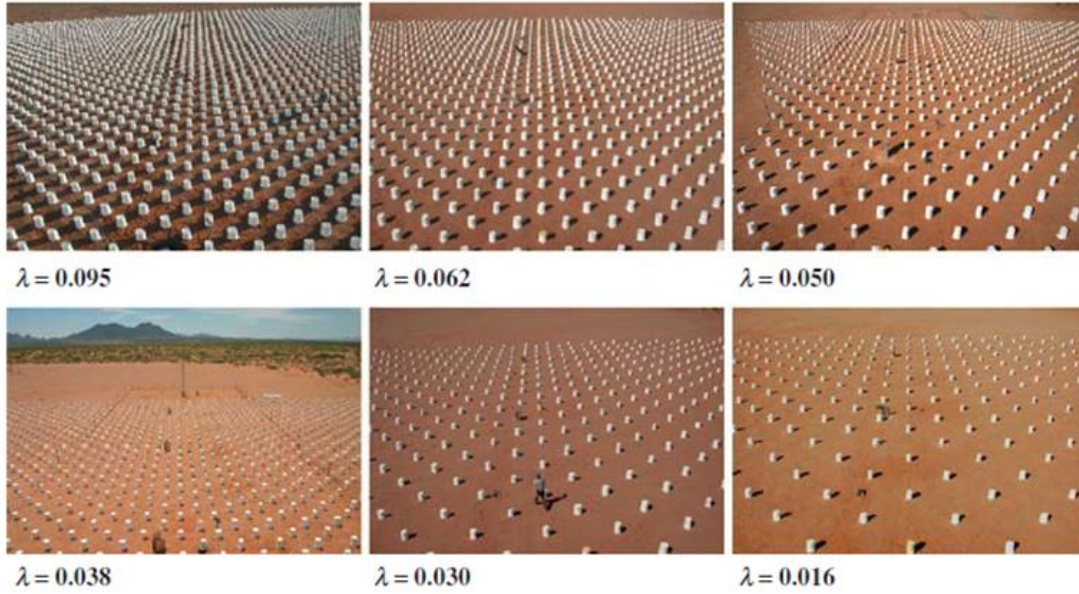
Fig.26.Images of the six roughness arrays used in the experiments [35]
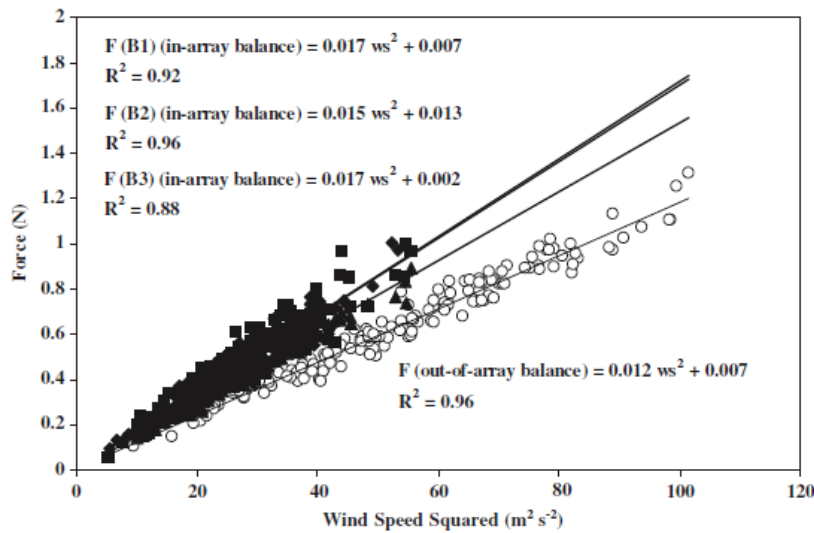
Fig.27 Typical force versus wind speed squared relationship [35]

The calibration for each measurement used 60 s intervals. It used to convert output to force on wind direction measured by the wind vane. Drag balance were used to measure the applied wind force within and upwind of the array on the elements. Here the references wind speed being 0.36m (the height of the roughness element), which is obtained by estimate the measured wind speed versus height relationship, as Fig 27 shown. The Drag coefficients (Cd_e) were also measured by the following equation.

$$Cd_e = \frac{F}{\rho_a\,A\,u_z{}^2} \tag{4}$$

Where Cd_e is the drag coefficient,

F is the force on the element (N),

A is frontal area of the element (m^2),

ρ a is air density (kg m-3),

U_z is wind speed (m s-1) at height z (m).

Calibration:

Before the experiment was conducted, the calibration of the instruments is necessary. Firstly, the instrument was put on a bench. A known weight mass was hanged on the point where the roughness element was fixed to the lever arm to establish the force versus output relationship. Considering that the wind direction is not perpendicular to the front face of the roughness element, the calibration relationships are developed for 5 ° intervals either side of the centerline of the element. According to the linear relationship between the output and the drag force, when the output data shown in the computer is correspond to the drag force which the known mass generated, the instrument was ready for experiments.

An example of the calibration relationships of the force balance is shown in Fig 28.
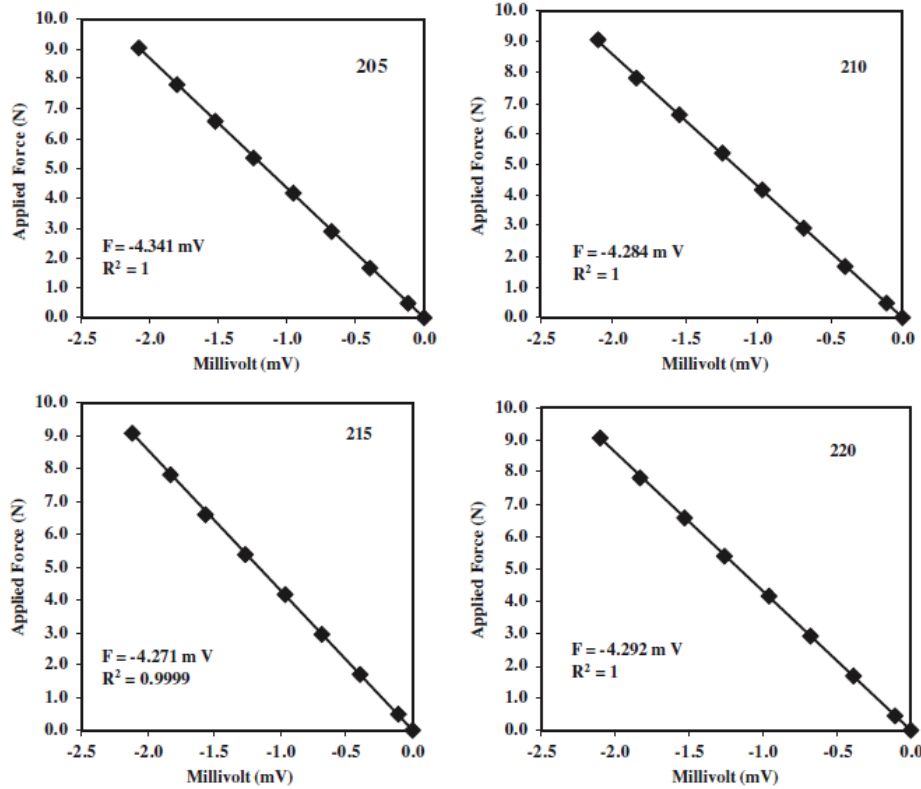
Fig28 Typical force versus mV relationships for 5 ° intervals for the force balances used in 2004.[35]

Development of this method:

This experiment was designed in an open area, not in wind tunnels. However, it is possible to perform it in wind tunnels as a develop method.

According to the size of roughness elements, the wind tunnel height should be at least 3times the buckets' height. The smaller size of buckets could be chosen. The wind tunnel dimension could be designed as like the experiment conducted in Gävle university wind tunnel laboratory.

Advantages:

1.   The drag force of each roughness element was obtained available. The characteristic of

each element located in different position was observed clearly. Such as the drag force in upstream was larger than that in downstream and the each drag force in different density arrays.

2.   The calibration process was easy relatively.

Disadvantages:

1.   A large open area (total area almost $10,000m^2$) was necessary because lots of roughness elements were used in the method.

2.   A great number of sensors were applied for measuring the drag force of each element and total drag force.

3.   It was complex and long process for changing the array densities among such many elements.

4.   Quite high cost used in this experiment from the view of economic.

5.   The calibration for each sensor was needed.

3.6 Thin-Oil-film techniques (indirect method)

Background:

The method oil-film interferometry was based on the behavior of an oil film (typically less than $10\,\mu m$) when shear stress acts on it. This technique has developed considerably in the past 10 years. Tanner and Blows first suggested the use of interferometry to determine the oil film thickness. Drag force could be obtained in wind tunnel by measuring the wall shear stress. Therefore, it was an indirect method for measuring drag force. Hence, it was necessary to

know that the relationship between wall shear stress and the thickness of an oil film in contact with the wall.

Description:

To describe the principle of this method, suppose a small oil droplet on a smooth wall. When it was exposed in the wind tunnel, a wedge like film would be formed. As the following picture shows;
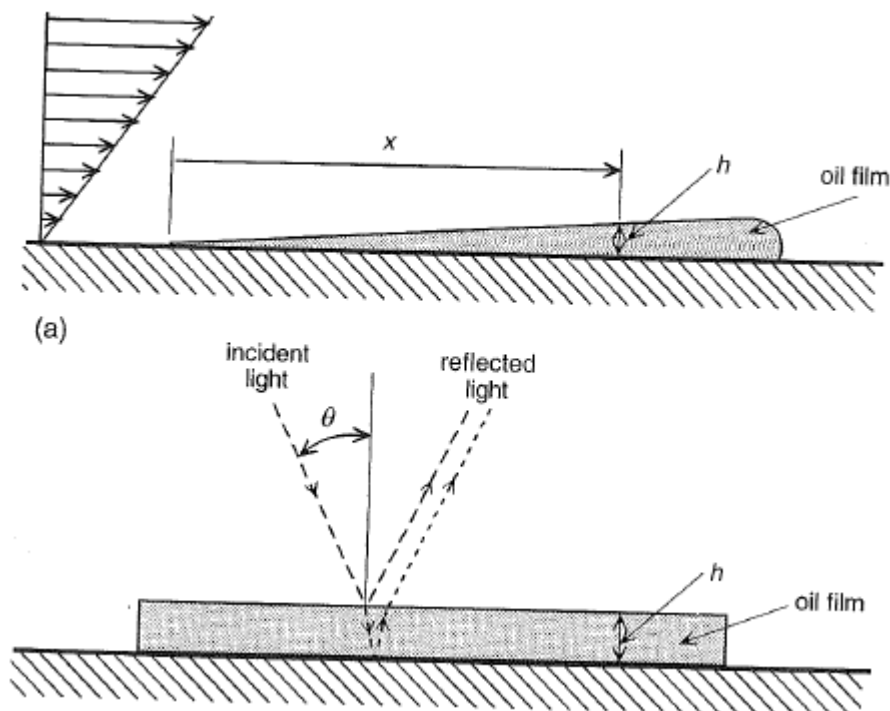
Fig.29.Sketches of (a) a stream wise cross-section of an oil film and (b) a span wise cross-section of the same film at a location x, also showing the incident and reflected light beams[36].

It is assumed that the oil flow was two dimensional, so the shear stress was uniform. Since the small film thicknesses, the effects of gravity, the pressure gradient and surface tension could

be neglected. The relationship among wall shear stress, local thickness h, and time t as follows;

$$\tau_w = \frac{\mu_{oil}x}{h(x,t)t}$$ (5)

Where,

τ_w is the wall shear stress,

μ_{oil} is the absolute viscosity of oil,

x is the displacement of oil drop,

h is the local thickness, and

t is the time.

The requirement of the light using here was from a sodium or mercury lamp, and the light directly on the film with a angle of incidence θ. According to the interferometry principle, there were two parts of lights are reflected. One was reflected off the oil surface, while the other entered the oil. Then the latter would be reflected off the wall and the second time through the oil film to enter the air again. The two reflected beams interfered with each other resulting dark and bright fringes [37] [39](*Fig.30.*).
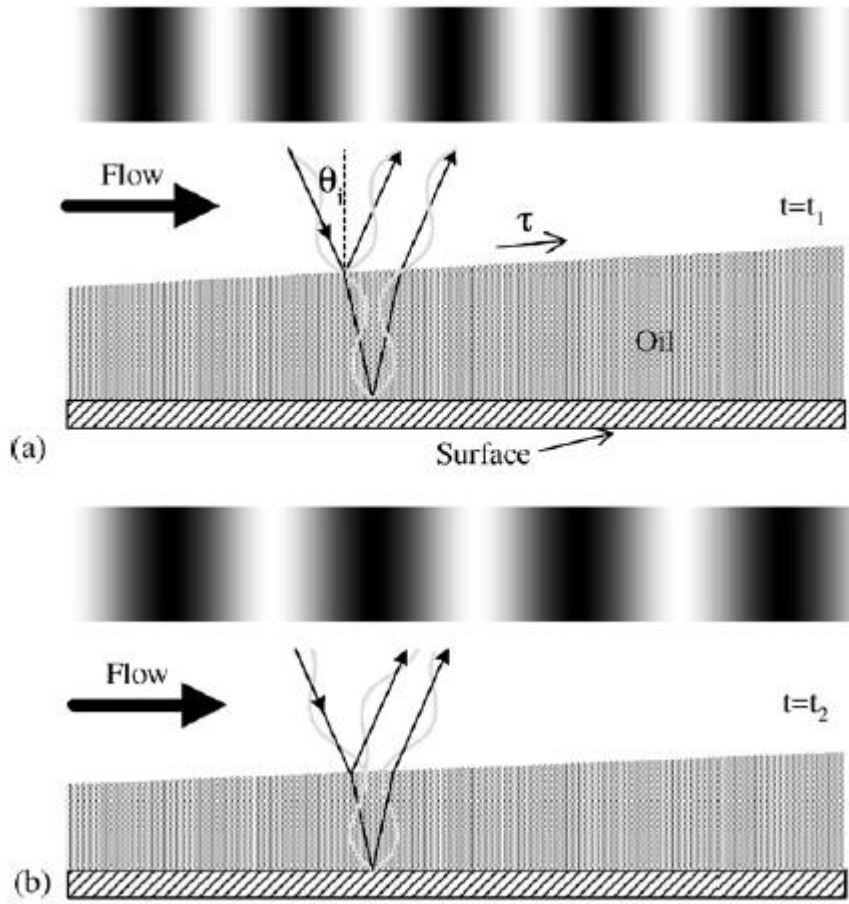
Fig.30. Interference fringes produced by Fizeau Interferometry:(a) Constructive interference produces bright bands,Whereas (b) destructive interference produces dark bands[38].

According to the basic interference optics, the film thickness could be obtained by following equation;

$$h(x, t) = \frac{\lambda \varphi}{4\Pi \sqrt{n_{oil}^2 - n_{air}^2 \sin^2 \theta}} \tag{6}$$

Where n_{oil} and n_{air} are the refractive indices of oil and air respectively,

and λ is the wavelength of the incident light [40] [41].

The dark fringes shows when the phase shift φ is an odd multiple of 2Π, and in contrast, the bright fringes shows when the phase shift φ is an even multiple of 2Π [42][43].

The components of the experiment as shown in *Fig.31*.
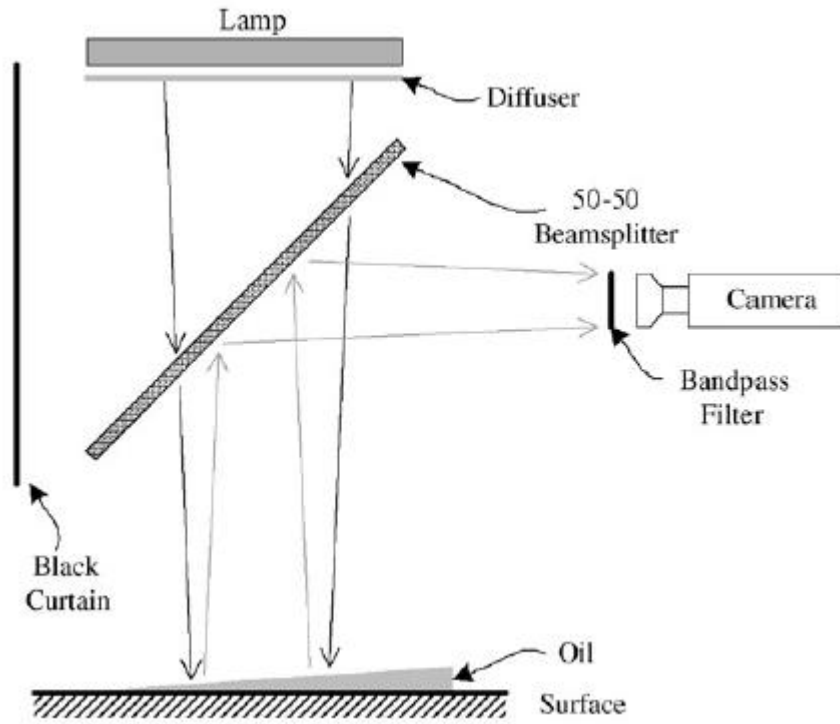
Fig.31. Image-based oil-film interferometry setup [38].

About the surface requirement, reflective surfaces and high indices of refraction are particularly attractive for interferometry. However, most aerodynamic test models are not made of such materials and rough surfaces are unsuitable for interferometry. Theory shows that a surface with an index of refraction n_s of 2.0 provides the optimum fringes [44]. A list of materials that are commonly considered for oil-film interferometry is given in *Table 2*.

Table 2. Characteristics for surfaces used in oil-film interferometry [38]

Material	Quality	n_s	Example references
SF 11 glass	Excellent	1.78	[68,77]
Mylar film	Good	1.67	[76,77,82]
Nickel	Good	1.6–2.0	[83]
Polished stainless steel	Acceptable		[73,84,85,80,77,76]
Polished aluminum	Poor	1.44	[86]

For light sources, He–Ne laser was used as the light sources in the beginning, since it is monochromatic and has a long coherence length. But it was proved that non-laser light source had more advantages than laser sources. Such as lower cost, lower electrical power consumption and higher optical power. In addition, their shorter coherence lengths could reduce speckle. Table shows the several light sources used in oil-film interferometry.

Table 3. Light sources used in oil-film interferometry [38]

Light source	Wavelength (nm)
He–Ne laser	632.8
Fluorescent lamps	Green—use with filter
Sodium lamp	589
Mercury lamp	435.8, 546.1
Xenon flash	Broadband—use with filter

Calibration is not needed because the data of shear stress is not obtained from the measurement directly, but through the calculation procedure.

Advantages:

1. This techniques have enhanced capabilities and greater accuracy compared to conventional shear-stress measurement.

<u>*Disadvantages:*</u>

1.   The requirement of specialized surfaces that provide the necessary reflection properties is difficult to be satisfied.

2.   Many factors needed to be considered when the model surface was chosen. Such as easily cleaned, chemically unreactive to oil and durability.

3.   It is cannot used to make fluctuating measurements.

3.7 Irwin sensor technique
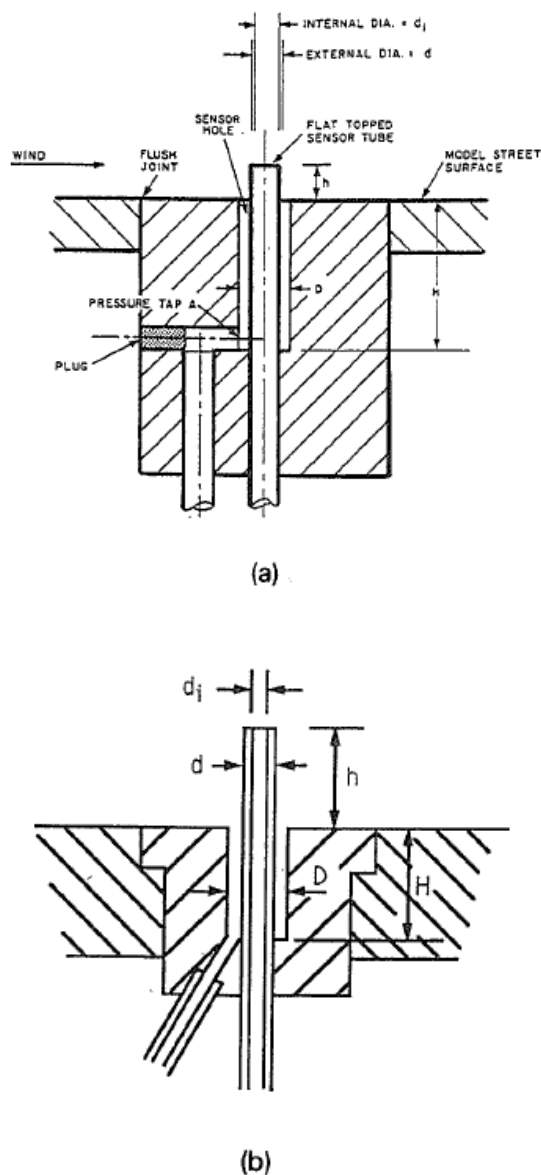
Fig 32. Sketches of the surface wind sensors:(a) designed by Irwin (b) reproduced in the current study [49]

Background:

Shear stress on the surface can be measured with Irwin sensors due to the relationship between shear stress and wind speed. Irwin proposed that surface wind flows can be measured by an omnidirectional pressure. Compared to other traditional measuring techniques, Irwin sensor is more accurate and convenient in wind-tunnel experiments.

The Irwin pressure transducer which generates a signal as a function of the pressure imposed. The signal is electrical.

Description:

As Fig 32 showed, (a) is the Irwin sensor original design with standard dimensions and (b) is the sensor made at the building Aerodynamics Laboratory of the Centre for Building Studies in Concordia University, Montreal. However, each sensor has almost same components, such as two brass tubes and a mounting base. And the two tubes have different positions, that is, one is protrudes out of the base as a probe and the other one is connected with a circular hole on the base around the probe[49].

The different pressures δp between the inlets of the two tubes are output of the sensor. The pressure difference and the wind speed Q can be related by the following equation:

$$Q= Av/h+B\sqrt{\delta p/\rho} = \alpha + \beta \sqrt{\delta p} , \tag{7}$$

Where h is the height of the sensor probe, ρ and v are the density and kinematic viscosity of air flow, A, B, α and β are constants depending upon flow characteristics, sensor dimensions, measuring height and other parameters.

According to the equation above, wind speed Q was proportional to pressure differences δp.

An example of the relationship between the output from an Irwin sensor and τ estimated from the vertical wind speed gradient is shown in Fig 33.
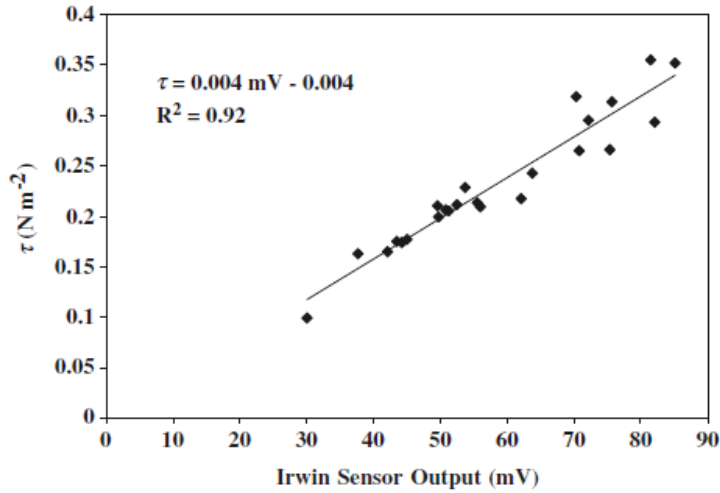
Fig 33. an example of the relationship between τ *estimated from the vertical wind speed profile and mV output from the Irwin sensor located exterior and upwind of a roughness array. [35]*

Obviously, the shear stress was proportional to wind speed. As the result of mentioned above, the wind speed and the pressure difference were linear relationship. Consequently, the shear stress was proportional to pressure variations.

Calibration:

The calibration of the Irwin sensors is according to the 10min average τ values and the associated 10min average mV output from the Irwin sensor pressure transducer. When the average shear stress was correspond with the output from the Irwin sensor, the sensor was ready and could be used.

Advantages:

1. The sensor can measure the low wind speeds higher than 3m/s.
2. It is easy to be calibrated.
3. Higher accurate and convenient than other traditional measuring techniques.

4. Conclusions

The technology of drag force measurements in contemporary ear has a significant elevation. From 1993, Maruyama installed an element floating on water to 2010 Mats Sandberg and Hans Wigö measured drag force in the wind tunnels with a standard load cell; from simple equipments to high precision equipments; the size of test section in wind tunnels also has become wide range of uses.

The total drag force acting on an element floating on water was measured directly using a strain gauge. The experiment was conducted in the wind tunnel at the Interdisciplinary Graduate School of Engineering Sciences, Kyushu University, Japan. The calibration of the system should be conducted carefully because of the precision. The top surface of the floating element must be at the same height as the surrounding tunnel floor. The space between the floating element and the tunnel floor was about 2mm on all sides. Furthermore, the calibration of the strain gauge was also important before the experiment was performed.

In 2006, the experiment measuring the shear stress using a mechanical device was conducted in the Department of Mechanical Engineering, Yamaguchi University. The roughness was arrayed on a floating element connected with the device. Because of the linear relationship between drag force and the displacement of the floating element, this method was widely desirable.

Compared to the floating element in water bath, the floating element in oil bath experiment which was conducted in EnElo, School of Engineering,, University of Surrey, UK was advanced relatively. Due to the character of the oil, high viscosity compared to water, there were more advantages in this method. The calibration before the experiment was performed was always necessary.

In 2010, the professors of Gävle University Sandberg M, Wigö H measured the drag force using the load cell in the wind tunnel. Different density of blocks was arrayed on the disc and

the turntable. The drag force acting on the blocks was measured by the load cell which was connected with the disc and mounted on a stable tripod on the floor of the laboratory hall. The system was calibrated with using a known mass (100grams), and calibration was needed if the blocks density was changed.

The individual drag force was available via the method was performed in an open area by John A.Gillies, William G.Nickling, James King in 2006. The Irwin sensor could measure the drag force of each roughness element due to the linear relationship between shear stress and the output from the Irwin sensor. The drag coefficient was obtained by extrapolating the measured wind speed versus height relationship.

The method of thin-oil-film techniques based on the interferometry of the oil film. The drag force was obtained according to the relationship between wall shear stress and the thickness of the oil film in contact with the wall. The experiment was carried out in wind tunnel and the small droplet oil on the smooth wall. In this method, the light source was an important factor.

In addition, from economic point of view, the floating elements in water bath and oil bath are more welcome, and also these two methods are easy to be conducted in a general environment, but water has lower viscosity, the damping oscillation of the floating element might affect the result during the experiment. On the other hand, the calibration procedures of both two methods are not complicated.

In contrast, the measurement using a mechanical device has relatively higher cost compared to the floating element in water bath and oil bath. Nevertheless, the high accuracy was the factor should be considered in this method.

Using the advanced method mentioned in the present thesis, the drag force of each element can be obtained directly. However, the cost of devices used in the method could be considered carefully, because the device has to be used in each element in the experiment. Additionally, the procedure of the calibration of each device is also an important factor in this method.

For the indirect method, the thin-oil-film was a good choice. In addition, there are high requirements for the surface of wall and the light source. Moreover, Irwin sensor provides higher accurate and reliable method in the shear stress measuring experiment.

Overall, choosing an appropriate method of drag force measurement in wind tunnels, many factors should be considered, such as, the aim, the cost, the environment, the complexity of procedure (including the calibration), the accuracy, the efficiency and so forth. So more investigations would be carried out in order to acquire reliable and accurate methods of drag force measurement in wind tunnels.

References

[1]   Aya Hagishima, Jun Tanimoto, Koji Nagayama, Sho Meno(2009) Aerodynamic Parameters of Regular Arrays of Rectangular Blocks with Various Gemetries. Boundary-Layer Meteorol 132:315-337.

[2]   Hurt, H.H.Jr. Aerodynamics for Naval Aviators. p.29

[3]   Clancy, L.J. Aerodynamics. Section 4.10

[4]   Massey, B.S. Mechanics of Fluids, section 10.8.2

[5]   Clancy, L.J. (1975) Aerodynamics Fig 5.24. Pitman Publishing Limited, London. ISBN 0-273-01120-0

[6]   Hurt, H. H. (1965) Aerodynamics for Naval Aviators, Figure 1.30, NAVWEPS 00-80T-80

[7]   Symon, Keith (1971). Mechanics (Third ed.). Addison-Wesley. ISBN 0-201-07392-7.

[8]   Edgeworth,, R.; Dalton, B.J.; Parnell, T.. "The pitch drop experiment". University of Queensland.

Retrieved 2009-03-31. A copy of: European Journal of Physics (1984) pp. 198–200.

[9]   Basic flight physics. Retrieved 16 October 2011

[10]   Motions of particles through fluids. Retrieved 16 October 2011.

[11]   French, A. P. (1970). Newtonian Mechanics (The M.I.T. Introductory Physics Series) (1st ed.). W W. Norton & Company Inc., New York. ISBN 393-09958-X.

[12]   "What is Lift?" NASA Glenn Research Center. Retrieved March 4, 2009.

[13]   McCormick, Barnes W. (1979): Aerodynamics, Aeronautics, and Flight Mechanics. p. 24, John Wiley & Sons, Inc., New York, ISBN 0-471-03032-5

[14]   P.Bradshaw. http://vonkarman.stanford.edu/tsd/pbstuff/tunnel/index.html

[15]   W.H.Rae and A.Pope. Low-Speed Wind Tunnel Testing. Wiley,New York,1984.

[16]   S.P. Parker. Fluid Mechanics Source Book. McGraw-Hill,New York,1987.

[17]   National Research Council Canada. Aerodynamics laboratory, 2002, available on-line: http://iar-ira.nrc-cnrc.gc.ca

[18]   NASA, Ames Research Center. Wind tunnels, 2003, available on-line:
        http://windtunnels.arc.nasa.gov

[19]   The Worthey Connection. The wind tunnel connection, 2001, available on-line:
        http://www.worthey.net/windtunnels/

[20]   P. Bradshaw. Experimental Fluid Mechanics. Pergamon, Oxford, UK, 1970.

[21]   P. Bradshaw and R.C.Pankhurst. The design of low-speed wind tunnels. In D.
        Kuechemann and L. H. G. Sterne, editors, Progress in Aeronautical Science, Vol. 5,
        Chap. 1,pp. 1-69. Pergamon, Press, Oxford, UK, 1964.

[22]   R. D. Mehta and P. Bradshaw. Design rules for small low speed wind tunnels.
        Aeronaut. J., 73:443-449, 1979.

[23]   R. Gordon and M.S. Imbabi. CFD simulation and experimental validation of a new
        closed circuit wind/water tunnel design. J. Fluids Eng., 120:311-318, 1998.

[24]   JetStream (2008). "Origin of Wind". National Weather Service Southern Region
        Headquarters.   http://www.srh.noaa.gov/jetstream//synoptic/wind.htm.   Retrieved
        2009-02-16.

[25]   Stokes, George (1851). "On the Effect of the Internal Friction of Fluids on the
        Motion of Pendulums". Transactions of the Cambridge Philosophical Society 9:
        8–106. Bibcode 1851TCaPS...9....8S

[26]   Reynolds, Osborne (1883). "An experimental investigation of the circumstances
        which determine whether the motion of water shall be direct or sinuous, and of the
        law of resistance in parallel channels". Philosophical Transactions of the Royal
        Society 174 (0): 935–982. doi:10.1098/rstl.1883.0029. JSTOR 109431

[27]   Rott, N. (1990). "Note on the history of the Reynolds number". Annual Review of
        Fluid   Mechanics   22   (1):   1–11.   Bibcode   1990AnRFM..22....1R.
        doi:10.1146/annurev.fl.22.010190.000245

[28]   Fluid mechanics tutorial No.3 Boundary layer theory

[29]   spanwise_variations_in_nominally_two-dimensional_rough-wall_boundary_layers

[30]   Maruyama T (1993) Optimization of roughness parameters for staggered arrayed
        cubic blocks using experimental data. J Wind Eng Ind Aerodyn 46&47:165-171.

[31]   Mochizuki S,Kameda T, Osaka H (2006) Self-preservation of a turbulent boundary

layer over d-type roughness. J Fluid Sci Tech 1:24-35

[32]   Gaudedt, L. and Winter, K, G (1973)   Measurements of the drag of some characteristic aircraft excrescences immersed in turbulent boundary layer, AGARD CP124.

[33]   Cheng H, Hayden P. Robins AG.Castro IP (2007) Flow over cube arrays of different packing densities. Journal of Wind Engineering and Industrial Aerodynamics 95:715-740

[34]   Buccolieri R., Sartoretto F., Giacometti A., Di Sabatino S., Leo L.S., Pulvirenti B., Sandberg M., Wigö H. (2010) Flow and pollutant dispersion within the Canal Grande channel in Venice via CFD techniques. Proc. 13th Int. Conf. on.

[35]   Gillies JA, Nickling WG, King J (2007) Shear stress partitioning in large patches of roughness in the atmospheric inertial sublayer. Boundary-Layer Meteorol 122:367-396.

[36]   Stavros Tavoularis (2005) Measurement in fluid mechanics. Page 340

[37]   H. H. Fernholz, G. Janke, M. Schober, P. M. Wagner, and D. Warnack. New developments and applications of skin-friction measuring techniques. Meas. Sci. Technol., 7:1396-1409, 1996.

[38]   J. W. Naughton and M.Sheplak. Morden developments in shear-stress measurement. Prog. Aerospace Sci., 38:515-570, 2002.

[39]   C. Mercer (Editor). Optical Metrology for Fluids, Combustion and Solids. Kluwer Academic, Dordrecht,The Netherlands, 2003.

[40]   L. H Tanner and L. G Blows. A study of the motion of oil films on surfaces in air flow, with application to the measurement of skin friction. J. Phys. E, 9:194-202, 1976.

[41]   J. D. Murphy and R. V. Westphal. The laser interferometer skin-friction meter: A numerical and experimental study. J. Phys. E, 19:744-751, 1986.

[42]   R. V. Westphal, W. D. Bachalo, and M. H. Houser. Improved skin friction interferometer. NASA Tech. Memo.88216. NASA Ances Research Center, Moffett Field, CA, 1986.

[43]   D. M. Driver. Application of oil film interferometry skin-friction to large

wind-tunnels. AGARD CP-601, Paper 25. Advisory Group for Aerospace Research and Development, Paris, 1997.

[44]   Zilliac G. Further developments of the fringe-imaging skin-friction technique. Tech. Rep. NASA/TM 110425, NASA-Ames Research Center, December 1996.

[45]   Fundamentals of fluid mechanics SI Version

[46]   Measurement in fluid mechanics Stavros Tavoularis

[47]   website: http://www.sensorland.com/HowPage002.html

[48]   website:http://www.universalsemiconductor.com/mems_gas_sensor.htm

[49]   Hanqing Wu, Theodore Stathopoulos(1994) Further experiments on Irwin's surface wind sensor.   Journal of wind engineering and industrial aerodynamics 53:441-452.

Appendix

Flow over immersed bodies
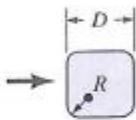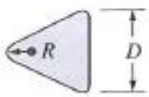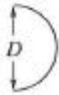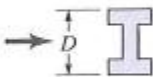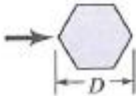
Shape	Reference area A (b = length)	Drag coefficient $C_D = \dfrac{\mathcal{D}}{\frac{1}{2}\rho U^2 A}$	Reynolds number $Re = \rho U D / \mu$
Square rod with rounded corners	$A = bD$	R/D | C_D 0 | 2.2 0.02 | 2.0 0.17 | 1.2 0.33 | 1.0	$Re = 10^5$
Rounded equilateral triangle	$A = bD$	R/D | C_D (→) | (←) 0 | 1.4 | 2.1 0.02 | 1.2 | 2.0 0.08 | 1.3 | 1.9 0.25 | 1.1 | 1.3	$Re = 10^5$
Semicircular shell	$A = bD$	→ 2.3 ← 1.1	$Re = 2 \times 10^4$
Semicircular cylinder	$A = bD$	→ 2.15 ← 1.15	$Re > 10^4$
T-beam	$A = bD$	→ 1.80 ← 1.65	$Re > 10^4$
I-beam	$A = bD$	2.05	$Re > 10^4$
Angle	$A = bD$	→ 1.98 ← 1.82	$Re > 10^4$
Hexagon	$A = bD$	1.0	$Re > 10^4$

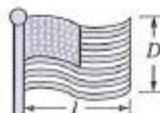*Figure1. Typical drag coefficients for regular two-dimensional objects*
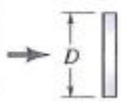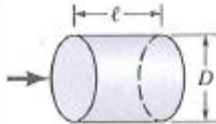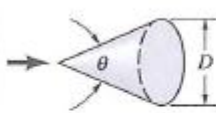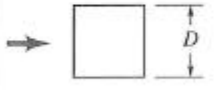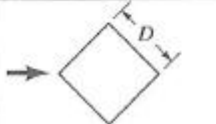
Shape		Reference area A	Drag coefficient C_D	Reynolds number $Re = \rho U D/\mu$
	Solid hemisphere	$A = \frac{\pi}{4}D^2$	→ 1.17 ← 0.42	$Re > 10^4$
	Hollow hemisphere	$A = \frac{\pi}{4}D^2$	→ 1.42 ← 0.38	$Re > 10^4$
	Thin disk	$A = \frac{\pi}{4}D^2$	1.1	$Re > 10^3$
	Circular rod parallel to flow	$A = \frac{\pi}{4}D^2$	ℓ/D | C_D 0.5 | 1.1 1.0 | 0.93 2.0 | 0.83 4.0 | 0.85	$Re > 10^5$
	Cone	$A = \frac{\pi}{4}D^2$	θ, degrees | C_D 10 | 0.30 30 | 0.55 60 | 0.80 90 | 1.15	$Re > 10^4$
	Cube	$A = D^2$	1.05	$Re > 10^4$
	Cube	$A = D^2$	0.80	$Re > 10^4$

Figure 2. Typical drag coefficients for regular three-dimensional objects
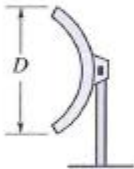
Shape	Reference area	Drag coefficient C_D
Parachute	Frontal area $A = \frac{\pi}{4}D^2$	1.4
Porous parabolic dish	Frontal area $A = \frac{\pi}{4}D^2$	Porosity: 0, 0.2, 0.5 / →: 1.42, 1.20, 0.82 / ←: 0.95, 0.90, 0.80 / Porosity = open area/total area
Average person	Standing / Sitting / Crouching	$C_D A = 0.8$ m^2 / $C_D A = 0.6$ m^2 / $C_D A = 0.2$ m^2
Fluttering flag	$A = \ell D$	ℓ/D: 1, 2, 3 → C_D: 0.07, 0.12, 0.15
Empire State Building	Frontal area	1.4
Six-car passenger train	Frontal area	1.8
Bikes / Upright commuter	$A = 0.5$ m^2	1.1
Racing	$A = 0.4$ m^2	0.88
Drafting	$A = 0.4$ m^2	0.50
Streamlined	$A = 0.46$ m^2	0.12

Figure 3. Typical drag coefficients for objects of interest